



Electric field distribution in relation to cell membrane electroporation in potato tuber tissue studied by magnetic resonance techniques



Matej Kranjc^a, Franci Bajd^b, Igor Serša^b, Mark de Boevere^c, Damijan Miklavčič^{a,*}

^a University of Ljubljana, Faculty of Electrical Engineering, Trzaska 25, 1000 Ljubljana, Slovenia

^b Institut "Jožef Stefan", Jamova cesta 39, 1000 Ljubljana, Slovenia

^c Pulsemaster, Rootveen 24, 5531 MB Bladel, The Netherlands

ARTICLE INFO

Article history:

Received 30 October 2015

Received in revised form 8 January 2016

Accepted 3 March 2016

Available online 12 March 2016

Keywords:

Electroporation

Magnetic resonance imaging

Magnetic resonance electrical impedance tomography

PEF treatment

ABSTRACT

Magnetic resonance electrical impedance tomography (MREIT) enables determination of electric field distribution during electroporation in which cell membrane permeability is increased by application of an external high electric field. In this study, MREIT was performed for the first time to predict electroporated areas in a pulsed electric field (PEF) treated vegetable tissue. The study was performed on potato tubers using different amplitudes of electric pulses and results were evaluated also by means of multiparametric MRI. MREIT determined regions of electric field distribution corresponded to visible darkened areas of the treated potatoes, as well to the results of multiparametric MRI. Results of this study suggest that MREIT could be used as an efficient tool for improving the effectiveness of PEF treatment applications.

Industrial relevance: This study presents a method capable of determining electric field distribution during PEF treatment using magnetic resonance electrical impedance tomography. The method has a practical value as it can potentially enable monitoring of the outcome of PEF applications which strongly depends on local electric field. Measurement of electric field distribution would enable detection of insufficient electric field coverage before the end of the PEF treatment, thus increasing and assuring its effectiveness.

© 2016 Elsevier Ltd. All rights reserved.

1. Introduction

In recent years, pulsed electric field (PEF) has been recognized as an efficient alternative to conventional approaches in numerous food processing applications (Barbosa-Cánovas, Pierson, Zhang, & Schaffner, 2000; Mahnič-Kalamiza, Vorobiev, & Miklavčič, 2014; Raso & Heinz, 2006; Vorobiev & Lebovka, 2010). PEF is based on electroporation, i.e. biological phenomena that increase permeability of a cell membrane when exposed to an electric field (Kotnik, Kramar, Pucihar, Miklavcic, & Tarek, 2012; Tsong, 1991; Yarmush, Golberg, Serša, Kotnik, & Miklavčič, 2014). In general, electroporation occurs when electric field strength exceeds a certain value, also known as electroporation threshold. If the field strength remains under irreversible electroporation threshold and the exposure time is sufficient, a cell membrane remains in a state of higher permeability for a period of time (Rols & Teissié, 1990). However, if the field strength exceeds irreversible electroporation threshold, irreversible electroporation occurs and the cell loses its homeostasis which leads to cell death (Jiang, Davalos, & Bischof, 2015). Consequently, applied electric field mostly determines the

outcome and the efficiency of electroporation applications, including food processing applications. Electric field strength in the range from several 100 V/cm to up to 1–2 kV/cm, i.e. moderate electric fields, are employed for extraction of water or solute out of plant tissues in applications such as juice extraction (Vorobiev & Lebovka, 2010), dehydration (Jaeger, Buechner, & Knorr, 2012), valuable compound recovery (Boussetta et al., 2011) and cryopreservation (Phoon, Galindo, Vicente, & Dejmek, 2008). Exposing treated plant tissues to high pulsed electric field, i.e. from 5 kV/cm to up to 50 kV/cm, is likely to cause irreversible damage of cells and for that reason can be used in applications such as liquid food product preservation (Buckow, Ng, & Toepfl, 2013; Raso, Calderón, Góngora, Barbosa-Cánovas, & Swanson, 1998; Toepfl, 2011).

A method capable of determining electric field distribution during the pulse delivery has a practical value as it can potentially enable monitoring of the outcome of PEF applications which strongly depends on local electric field (Miklavčič et al., 1998). Measurement of electric field distribution would enable detection of insufficient electric field coverage before the end of either reversible or irreversible PEF treatment, thus increasing and assuring its effectiveness. As the electric field distribution cannot be measured directly, we proposed an indirect approach. Magnetic resonance electrical impedance tomography (MREIT) proved to be an excellent candidate for determining an electric field distribution during electroporation (Kranjc, Bajd, Serša, & Miklavčič, 2011). The method enables reconstruction of the electric

* Corresponding author.

E-mail addresses: matej.kranjc@fe.uni-lj.si (M. Kranjc), franci.bajd@ijs.si (F. Bajd), igor.sersa@ijs.si (I. Serša), mark.deboevere@pulsemaster.us (M. de Boevere), damijan.miklavcic@fe.uni-lj.si (D. Miklavčič).

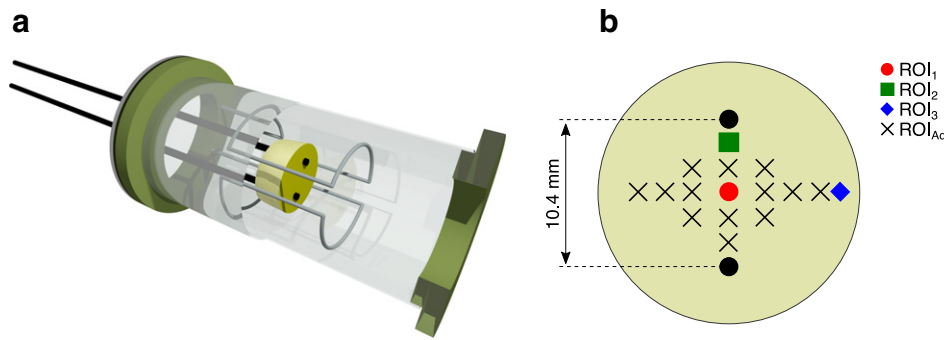


Fig. 1. Potato tuber sample with inserted needle electrodes placed in a MR microscopy probe (a), schematic axial cross-section through the potato sample with indicated three ROIs where multiparametric analysis was performed (b).

field distribution by measurement of an electric current density distribution and electrical conductivity of the treated subject during the application of electric pulses using MRI followed by numerical data analysis. MREIT has advanced rapidly in the last decade, especially in electrical conductivity imaging of biological tissues (Kim et al., 2009; Seo & Woo, 2014). MREIT enables determination of an electric field distribution in situ while taking into account changes that occur in the tissue due to electroporation. We demonstrated a successful reconstruction of the electric field distribution during electroporation in an agar phantom (Kranjc et al., 2011), ex vivo animal tissue (Kranjc, Bajd, Serša, & Miklavčič, 2014; Kranjc, Bajd, Serša, Woo, & Miklavčič, 2012), in silico (Kranjc et al., 2012) and in mouse tumor in vivo (Kranjc et al., 2015).

In this study, MREIT was performed for the first time to predict electroporated areas in a PEF treated vegetable tissue. MREIT was followed by multiparametric MR imaging including ADC and T_2 mapping that enabled dynamical follow-up of tissue changes after the PEF treatment. Our study was performed on potato tubers since PEF treatment is already well established in potato industry for reducing cutting forces, oil uptake and browning during frying (Ignat, Manzocco, Brunton, Nicoli, & Lyng, 2014). Besides apple tissue (Grimi, Mamouni, Lebovka, Vorobiev, & Vaxelaire, 2011), potato tuber is found to be appropriate for studying electroporation effects due to a possible additional visual discern of electroporated areas that become distinctively darker hours after the treatment (Hjouj & Rubinsky, 2010; Ivorra, Mir, & Rubinsky, 2009). As the applied electric field often results in non-uniform changes of cell viability due to potato tuber microstructure (Faridnia, Burritt, Bremer, & Oey, 2015) a method that would allow monitoring of the electric field distribution in the treated tubers during the PEF treatment would be of a great value.

2. Material and methods

2.1. Raw material handling

Yellow-fleshed potato tubers (*Solanum tuberosum*) cultivar “Agata” were purchased at the local supermarket (Ljubljana, Slovenia) and stored at 4 °C in the dark closed refrigerated chamber until used, i.e. less than 2 days. All of the potato tubers used in this study were from the same batch and free from any external damage.

2.2. Experimental setup

From the potato a disc-like sample measuring 21 mm in diameter and 2 mm in height was sliced and then placed in an acrylic glass container. As in our previous ex vivo studies (Kranjc et al., 2014) two cylindrically shaped, i.e. needle electrodes, were inserted in the potato sample. The electrodes were made of platinum–iridium, their diameter was 1 mm and they were inserted at a distance of 10.4 mm (see Fig. 1b). After the insertion, the electrodes were connected to an electric pulse generator, which was triggered by an MRI spectrometer synchronously

with the Current Density Imaging (CDI) pulse sequence. The sample was then inserted in a 25 mm MR microscopy probe inside a horizontal-bore superconducting MRI magnet (Fig. 1a). Each PEF treatment experiment was performed on a different fresh potato sample to ensure identical initial conditions in all experiments.

The feasibility study of monitoring electric field distribution during the application of electric pulses was performed on 15 potato tubers that were divided in two groups as shown in Table 1. Potatoes from group 1 and 2 were subjected to the electric pulses and to MREIT for reconstruction of electric field distribution inside the tubers. Electroporated areas in the potatoes from group 1 were evaluated by digital photographs taken 18 h after the PEF treatment, while the potatoes from group 2 were evaluated by dynamical multiparametric MRI. The photographs were taken by a digital camera Olympus XZ-1 (Olympus Corporation, Tokyo, Japan) with settings for exposure time (1/125 s) and aperture ($f/2.5$) kept the same for all samples. The PEF treated potatoes of both groups were compared by electric field distributions and the corresponding electroporated areas as obtained by MREIT analysis. In potatoes from group 2 regions of interest were used for assessment of electroporation treatment effects. The regions measure 5×5 pixels, i.e. 2.3×2.3 mm, and were placed: ROI₁ in the center between the electrodes, ROI₂ in proximity of the electrodes and ROI₃ in the outer region (Fig. 1b). Additional regions of interests (ROI_{Ad}) were introduced in determination of correlation between T_2 values and values of electric field.

2.3. Electroporation protocol

Electroporation treatment of potatoes was performed by applying two sequences of four high voltage electric pulses with a duration of 100 μ s, a pulse repetition frequency of 5 kHz and with an amplitude of 500 V, 750 V and 1000 V for samples group 1 and 750 V for samples from group 2. The electric pulses were delivered between the electrodes by an electric pulse generator Cliniporator Vitae (IGEA, Carpi, Italy).

2.4. Magnetic resonance imaging: current density imaging complemented by multiparametric MRI

The MR imaging was performed on a MRI scanner consisting of a 2.35 T (100 MHz proton frequency) horizontal bore superconducting

Table 1
Two groups of potato tubers used in the study.

	Group 1	Group 2
Number of samples	8	7
Names of samples	C1.1, C2.1 (control) P1.1–P1.6 500 V (P1.1, P1.2)	C2.1–C2.4 (control) P2.1, P2.2, P2.3
Amplitude of applied el. pulses	750 V (P1.3, P1.4) 1000 V (P1.5, P1.6)	750 V (P2.1, P2.2, P2.3)
Evaluation of electroporated area	Digital photography	Multiparametric MRI

Table 2
MRI parameters of the used pulse sequences.

Sequence parameters	ADC mapping	T_2 mapping	CDI
Pulse sequence	PFG SE	Multiecho SE	CDI RARE
Field of view [mm ²]	30 × 30		30 × 30
Imaging matrix	128 × 128		64 × 64
Resolution [μm ²]	234 × 234		469 × 469
Slice thickness [mm]	4		4
Signal averages	2	2	2
Number of echoes	1	8	64
Echo/interecho time [ms]	34	11:11:88	2.64
Repetition time [s]	1.035	1.930	10
b-Values [s/mm ²]	0, 240, 580, 1150	/	/
Scan time [min]	18	8	0.3

magnet (Oxford Instruments, Abingdon, United Kingdom) equipped with a Bruker micro-imaging system (Bruker, Ettlingen, Germany) for MR microscopy with a maximum imaging gradient of 300 mT/m and a Tecmag Apollo spectrometer (Tecmag, Houston TX, USA).

All samples exposed to electric pulses were treated inside the MRI magnet to enable treatment monitoring by means of electric field mapping. The mapping was enabled by CDI, which is an MRI method that enables imaging of current density distribution inside conductive samples (Joy, Scott, & Henkelman, 1989; Serša, Jarh, & Demsar, 1994). Briefly, in CDI, maps of image signal phase shift are acquired after application of electric current pulses to the sample. The phase shift is proportional to the average magnetic field change in the sample (in the direction of the static magnetic field) caused by currents flowing through the sample. Vector components of the induced magnetic field change can be obtained from the phase shift stored in the acquired images. Once these are known, electric current density in the sample can be calculated from the magnetic field change vector maps using Ampere's law. In the study two-shot RARE version of the CDI sequence was used. The sequence enabled image acquisition in just two signal excitations, thus

reducing the number of applied electric pulse trains to two for acquisition of one image.

Samples from group 2 were dynamically monitored by multiparametric MRI protocol. The protocol consisted of diffusion-weighted imaging (DWI) based on a pulsed gradient spin-echo (PGSE) sequence (Stejskal & Tanner, 1965) for the ADC mapping and a multi-spin-echo (MSE) imaging sequence based on the Carr–Purcell–Meiboom–Gill (CPMG) multi-echo train (Carr & Purcell, 1954) for the T_2 mapping. DWI and MSE images were taken every 45 min until 12 h after the PEF treatment. Analysis of multiparametric MRI data was performed as described previously in (Vidmar, Kralj, Bajd, & Serša, 2015). The imaging parameters of the sequences are given in Table 2.

2.5. Magnetic resonance electrical impedance tomography

Electric field distribution in a potato tissue during application of electric pulses was obtained by means of MREIT, which is a CDI-based imaging method (Kranjc et al., 2011, 2014). Electric field in the sample during application of electric pulses can be reconstructed from CDI data by a mathematical algorithm based on solving Laplace's equation. In the reconstruction, the corresponding Neumann and Dirichlet boundary conditions are considered for the sample geometry on the outer sample boundary and on the surface of the electrodes, respectively (Khang et al., 2002). Laplace's equation was solved iteratively using the finite element method with the numerical computational environment MATLAB 2015a (MathWorks, Natick, MA) on a desktop PC (Windows 8, 3.5 GHz, 32 GB RAM).

2.6. Finite element method simulation

Electric field distribution obtained by means of MREIT was compared to the results of the finite element method simulations for the same sample/electrode configuration. Geometries of potato tuber models were based on potato samples of group 1, while positions of

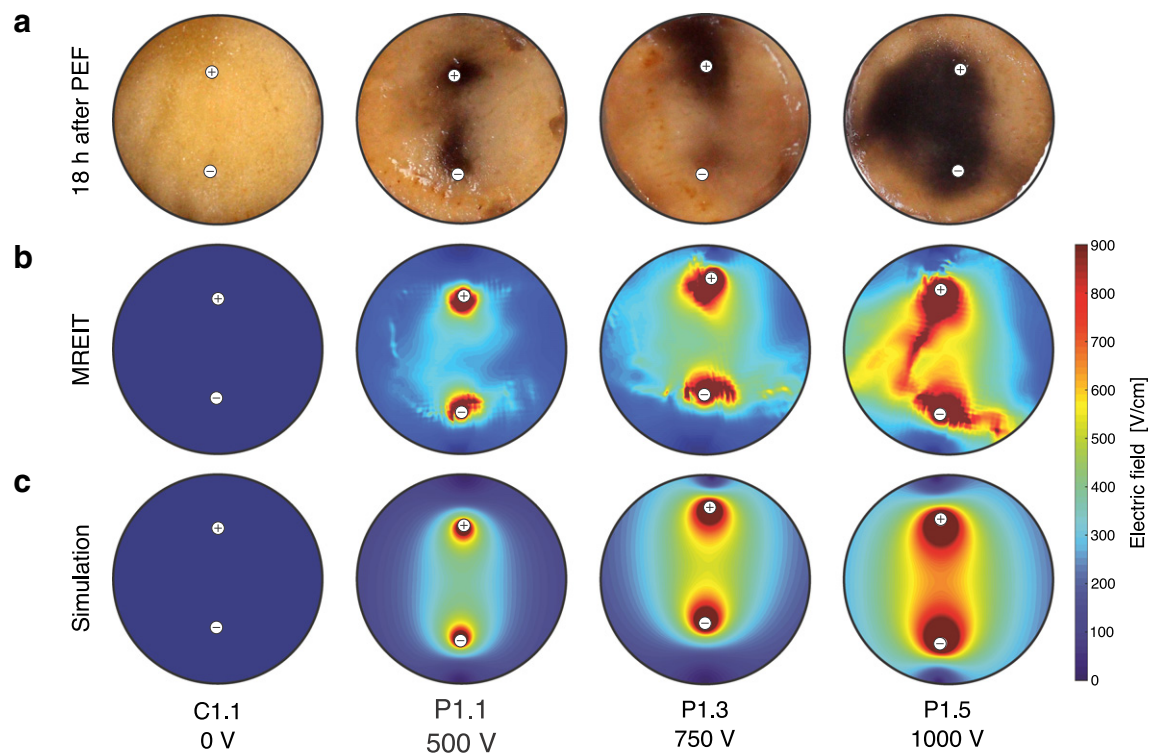


Fig. 2. Digital photographs of three potato tubers from group 1 and one potato from the control group taken 18 h after the PEF treatment (a), measured electric field distributions during the PEF treatment (b) and simulations of the electric field distributions using the finite element method (c). Potato tubers were subjected to electric pulses of amplitudes 0, 500, 750 and 1000 V.

the electrodes were determined from their MR images. Simulations of electric field distributions were performed for applied electric pulses of amplitudes 0 V, 500 V, 750 V and 1000 V. The model incorporated electric field dependent electrical conductivity that was taken from (Ivorra et al., 2009). Simulations were done in the computational environment MATLAB 2015a and its Partial Differential Equation Toolbox running on the same desktop PC as noted previously.

2.7. Statistical analysis

All results were analyzed and statistically described using commercial software MATLAB 2015a and its Statistics Toolbox. Correlation (r) between T_2 values and electric field intensity was evaluated with linear Pearson correlation analysis. Statistical significance of differences between groups of data were evaluated using Student t-test.

3. Results

A comparison of digital photographs of treated potatoes of group 1 taken 18 h after application of electric pulses and the corresponding measured and simulated electric field maps is shown in Fig. 2. The darkened region in the treated potatoes is a result of oxidation that began immediately after the treatment. The extent of regions with high electric field in the measured electric field maps corresponds to the results of the simulations, while the electric field distribution deviates from the simulated one due to local conductivity variations of the potato tissue.

ADC and T_2 maps at four different times after the PEF treatment (0, 140, 320 and 500 min) of three different samples of group 2 are shown in Figs. 3 and 4, respectively. From the ADC maps in Fig. 3 we can observe gradual reduction of ADC values in the region between the electrodes with time after the treatment. In addition, a positive correlation between the ADC increase and electric field in the sample during the treatment can be seen as well; this is best seen immediately after the treatment (0 min). The effect of the treatment is more pronounced in T_2 maps in Fig. 4. In the maps, T_2 values in the region between the electrodes, where electric field was high, are almost doubled (240 vs. 120 ms) in comparison to the values in the outer regions of the sample, where the treatment had no effect. From the T_2 maps we can observe gradual reduction of T_2 values in the region between the electrodes with time after the treatment. In both sets of maps, ADC in Fig. 3 and T_2 in Fig. 4, the effect of the treatment was considerably higher for the samples P2.1 and P2.2 than for the sample P2.3.

More precise analysis of the time course of changes in ADC and T_2 values after the PEF treatment of samples from group 2 is shown in Fig. 5. The analysis includes all measured time points of all three samples of group 2 taken from images in Figs. 3 and 4 for the three selected regions of interest. Average value \pm standard deviation of measured electric field intensity in regions of interest were 406 ± 12 V/cm, 829 ± 256 V/cm and 167 ± 6 V/cm for ROI₁, ROI₂ and ROI₃, respectively. Again, the observed effect of the PEF treatment on the change of ADC and T_2 values was much higher for the samples P2.1 and P2.2 than for the sample P2.3 and changes of ADC values were less significant than of T_2 values. The largest change of T_2 values was obtained in the proximity of the electrodes (ROI₂), where T_2 changed from 380 to 240 ms for

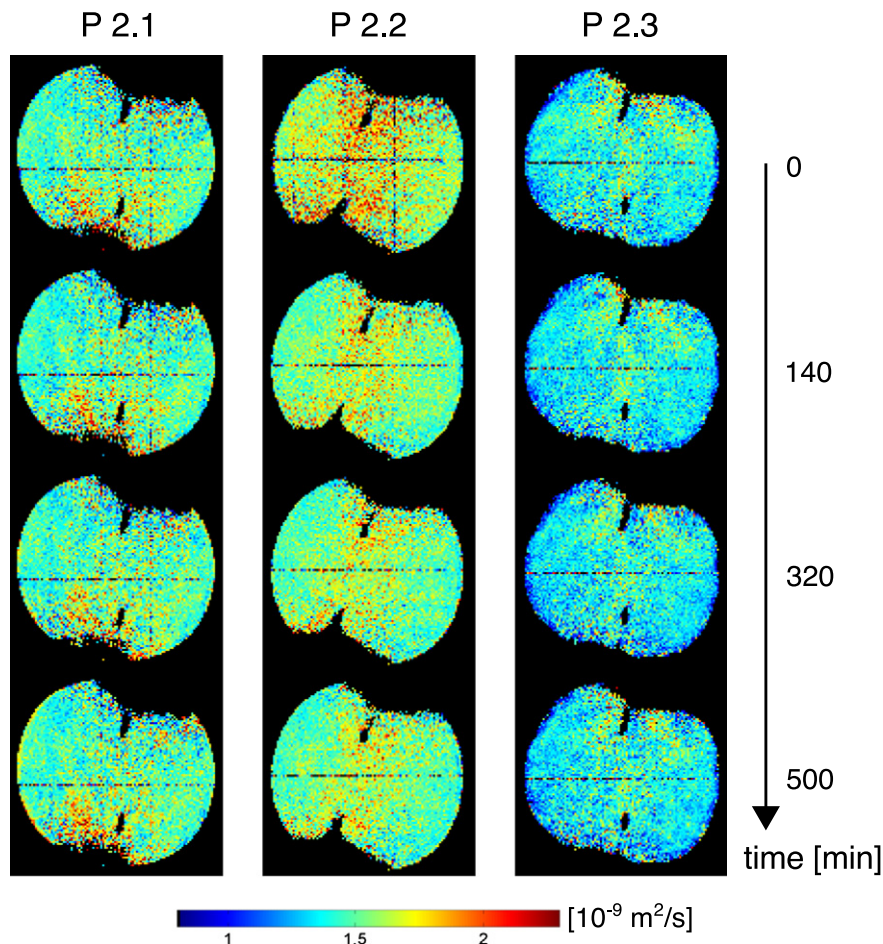


Fig. 3. Selected ADC maps acquired at four different times after (0, 140, 320 and 500 min) application of electric pulses of amplitude 750 V for three different examined potato samples (P2.1, P2.2, P2.3). The treated potato tissue gradually exhibits a reduction of ADC values in the region between the inserted electrodes.

the sample P2.1 and from 370 to 220 ms for the sample P2.2. The change was much lower for the region in the center between the electrodes (ROI_1) and was almost negligible in the outer region (ROI_3). In Fig. 5, the background at a given time point was colored gray if the difference between the values of ROI_1 and ROI_3 was statistically significant. Correlation between T_2 values and electric field values in ROI_{Ad} is shown in Fig. 6. A clear cut can be observed at 400 V/cm. Two different positive correlations for $E > 400$ V/cm were obtained, for T_2 values in ROI_{Ad} 45 min ($r = 0.84, p < 0.001$) and 12 h ($r = 0.71, p < 0.001$) after application of electric pulses. Weak linear relationship was obtained for T_2 values in ROI_{Ad} exposed to electric field ranging from 200 to 400 V/cm. Average T_2 value \pm standard deviation of potatoes exposed to electric field ranging from 200 to 400 V/cm was 139 ± 13 ms while for untreated potatoes (C2.1–C2.4) average T_2 value was 94 ± 15 ms.

4. Discussion

The aim of this study was to test feasibility of MREIT to predict an outcome of the PEF treatment of potato tubers. The study was performed using different amplitudes of electric pulses and the results of the treatment were evaluated by digital photography as well as by means of multiparametric MRI.

Results of group 1, i.e. treated potatoes that were evaluated by digital photography, indicate correspondence between electric field distributions obtained by MREIT (Fig. 2b) and darkened areas of the treated potatoes as shown in photographs (Fig. 2a). The darkened regions of the treated potatoes are result of the oxidation process of phenolic compounds under the action of an enzyme polyphenol oxidase (PPO,

phenolase). The darkened regions of the treated potatoes are good indicators for the efficiency of the PEF treatment since the start of the reaction is linked to a breakdown of cell membrane integrity and leakage of polyphenol oxidase.

Interestingly, electric field was not distributed symmetrically as in the simulated patterns of the electric field distribution. The effect was most pronounced at 1000 V amplitude. The origin of this asymmetric electric field distribution is due to heterogeneous potato structure (Faridnia et al., 2015) as well as its heterogeneous electrical conductivity, which resulted in an asymmetric distribution of the electric field. According to previous studies related to PEF treatment of potatoes, electrical conductivity of untreated potato tubers is considered homogeneous and with the application of electric pulses conductivity starts to increase following the sigmoid function (Ivorra et al., 2009). However, even with an electric field dependent conductivity, the electric field should be distributed symmetrically, similar to electric field distributions obtained by simulations in Fig. 2c. In our results obtained by MREIT, electric field distributions in potatoes were not symmetrical, suggesting that electrical conductivity of potatoes was heterogeneous even before the application of electric pulses. Interestingly, differences between the simulated electric field distribution and the electric field distribution obtained by MREIT are becoming more distinct with a higher amplitude of applied electric pulses.

In our study, multiparametric MRI was found a suitable tool for a characterization of induced tissue changes due to application of electric pulses. These are associated with changes of water environment in treated plant tissue (Finley, Schmidt, & Serianni, 1990). More specifically, PEF treatment results in a cell membrane poration and possibly also

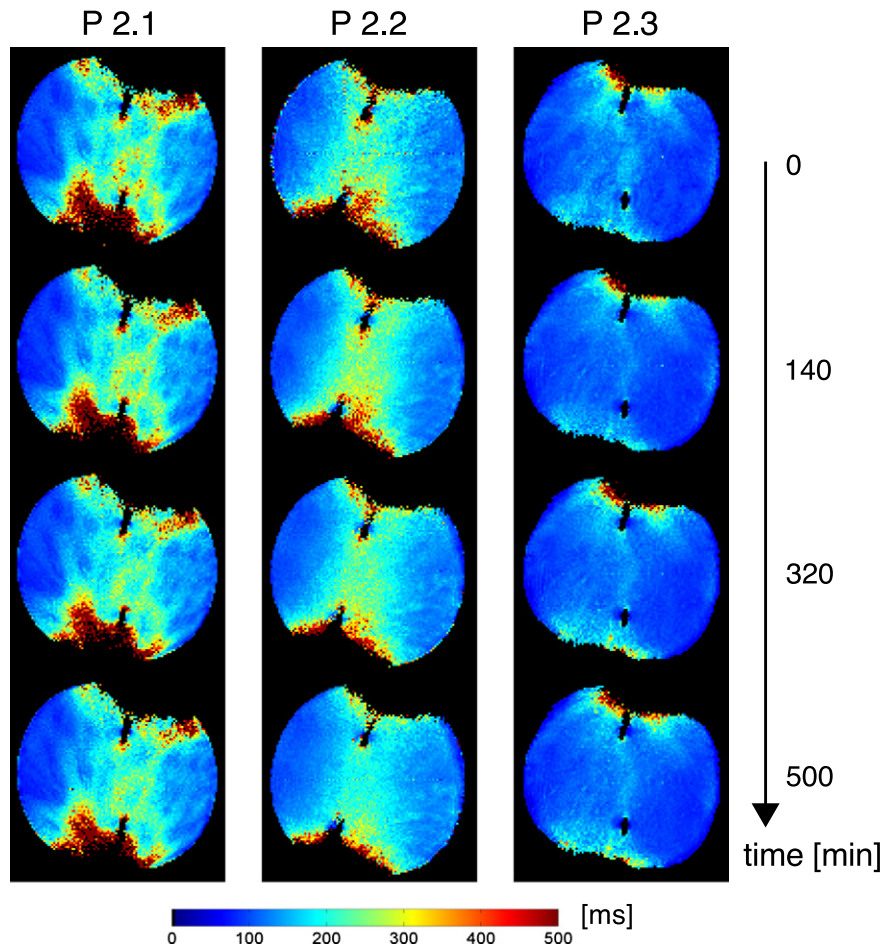


Fig. 4. Selected T_2 maps acquired at four different times after (0, 140, 320 and 500 min) application of electric pulses of amplitude 750 V for three different examined potato samples (P2.1, P2.2, P2.3). The treated potato tissue gradually exhibits a reduction of T_2 values in the region between the inserted electrodes.

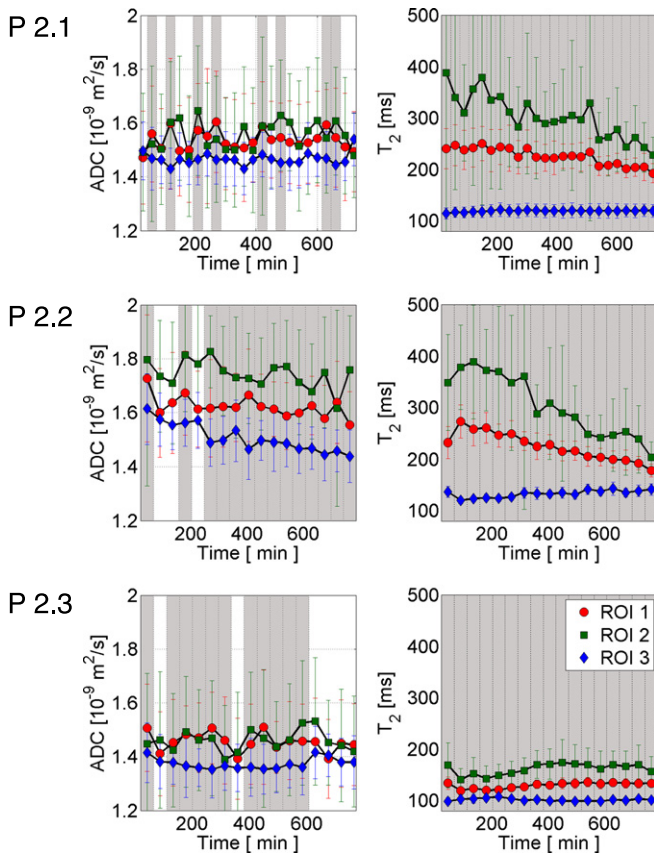


Fig. 5. Average maps of ADC and T_2 as a function of time in three potato tubers from group 2 (P2.1, P2.2, P2.3) in the potato center (ROI 1), in potato tissue close to the inserted electrode (ROI 2) and in unaffected potato tissue (ROI 3). Significant differences ($p < 0.05$) between the values corresponding to ROI 1 and ROI 3 are marked by gray background color.

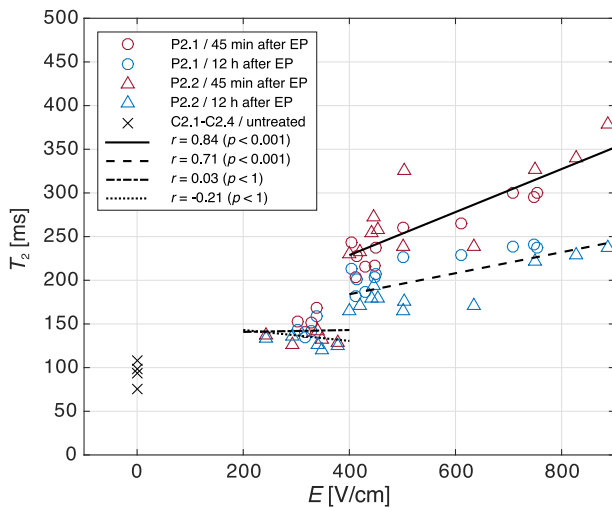


Fig. 6. Scatterplot of T_2 values and electric field values for two potatoes; P2.1 (marked with circles) and P2.2 (marked with triangles). T_2 values were obtained 45 min (red colored markers) and 12 h (blue colored markers) after electroporation (EP). Linear regression line was determined for values obtained 45 min (black solid line) and 12 h (dashed line) after EP in both potatoes for electric field values higher than 400 V/cm. For values lower than 400 V/cm additional two regression lines were determined, one for values obtained 45 min (dash-dotted line) and one for 12 h (dotted line) after EP. Values of T_2 for untreated potatoes (potatoes C2.1–C2.4) are marked with black crosses at 0 V/cm. Average standard deviation were 105 ms and 69 ms for potato sample P2.1 and P2.2, respectively.

in a electroporation of membranes of larger cell organelles followed by a release of intracellular liquid in the extracellular space. In addition, the treatment may also result in cell wall deformation and consequently in a change of extracellular space (Janositz, Noack, & Knorr, 2011). The release of intracellular liquid is associated with both, an increased extracellular water content and ion leakage, which have opposite effects on T_2 relaxation time. In our study, we observed T_2 increase which indicates a dominant effect of water release over ion leakage. It was also detected that after the PEF treatment the T_2 relaxation time decreased, which can be attributed to a water drainage (Ersus & Barrett, 2010). It was expected that the PEF treatment would have a bigger effect also on ADC of the treated potato tissue. However, the observed changes were negligible and were significant only with one examined sample (P2.2). This result could be explained by a rigid structure of cell walls in plant tissues that prevent substantial changes between intra- and extra-cellular spaces which largely determine ADC in animal tissues (van Everdingen, van der Grond, Kappelle, Ramos, & Mali, 1998).

As shown in Fig. 6, T_2 values in potatoes are scattered in three groups. Lowest values of T_2 , i.e. 94 ± 15 ms, were measured in untreated potato tubers ($E = 0$ V/cm) and were consistent with results from others studies (Nott, Shaarani, & Hall, 2003). Next scatter of T_2 values with the mean value of 139 ± 13 ms was obtained in areas of potatoes exposed to an electric field ranging from 200 V/cm to 400 V/cm. Values of T_2 were significantly different compared to untreated potatoes ($p < 0.001$), suggesting that electric field resulted in permeabilization of cells membrane and in the release of water content from potato cells to extracellular space. Values of T_2 and consequently the amount of extracellular water, however, have not changed significantly within 12 h. Third scatter of T_2 values was measured in areas of potato exposed to an electric field higher than 400 V/cm. Here, however, T_2 values were linearly increasing with the electric field, hence the amount of released water increased with the intensity of electric field. In contrast to results below 400 V/cm, the amount of extracellular water decreased with time (for easier comparison only T_2 values 45 min and 12 h after electroporation are presented in Fig. 6). Since the electric field value of 400 V/cm distincts two trends of T_2 values, one can speculate that two distinct electroporation processes were induced by an electric field of lower and higher value of 400 V/cm, i.e. reversible below 400 V/cm and irreversible electroporation above 400 V/cm. Obtained range of field strength for reversible electroporation (between 200 and 400 V/cm) is in agreement with the study by Galindo et al. in which reversible electroporation was demonstrated by propidium iodide staining of cell nucleus (Galindo et al., 2009) using comparable total electric field exposure time (1 ms) as in our study (800 μ s). Cell viability study also showed that field strength lower than 400 V/cm mostly does not influence the tuber cells whereas increased cell death was observed when higher field strengths were applied. Also, field strengths higher than 400 V/cm are reported to have a considerable impact on potato tuber microstructure, leakage of ion (Faridnia et al., 2015) and breakdown of the membrane (Angersbach, 2000). It seems that reported significant changes also correspond to changes of T_2 values as presented in our study.

Our study additionally confirms that the electric field determines the outcome and the efficiency of the electroporation process and that the proposed method of monitoring electric field distribution using MREIT could become an efficient tool for monitoring PEF treatment in various PEF applications. Since monitoring is performed during pulse delivery, the determined electric field distribution takes into account all heterogeneities and changes, which occur in the treated tissue. Moreover, the latest development in CDI sequence design for applications in electroporation enables electric field mapping already after just two applied pulses (Serša, Kranjc, & Miklavčič, 2015). This near-real-time information can also be used for fine adjustments of PEF treatment parameters, such as amplitudes of electric pulses or changing their number, during the PEF treatment. The adjustments are essential for an on-line

improvement of the treatment effectiveness. Still, before implementation of proposed method to existing PEF processes MREIT algorithm will have to be modified for the use with electrodes placed outside of potato tuber.

5. Conclusion

Monitoring of electric field distribution during the application of electric pulses in a potato tissue by means of magnetic resonance electrical impedance tomography is described and investigated experimentally. Magnetic resonance electrical impedance tomography determined regions of electric field distribution corresponded to darkened areas of the treated potatoes on digital photographs. Furthermore, the electric field distribution correlated well with the results of multiparametric MRI given by sequential ADC and T_2 mapping. Results of this study suggest that MREIT could be used as an efficient tool for improving the effectiveness of PEF treatment applications.

Acknowledgments

This study was supported by the Slovenian Research Agency (ARRS) under Grant P2-0249 and conducted within the scope of the Electroporation in Biology and Medicine European Associated Laboratory (LEA-EBAM). This manuscript is a result of the networking efforts of the COST Action TD1104 (www.electroporation.net).

References

- Angersbach, A. (2000). Effects of pulsed electric fields on cell membranes in real food systems. *Innovative Food Science & Emerging Technologies*, 1(2), 135–149. [http://dx.doi.org/10.1016/S1466-8564\(00\)00010-2](http://dx.doi.org/10.1016/S1466-8564(00)00010-2).
- Barbosa-Canovas, G. V., Pierson, M. D., Zhang, Q. H., & Schaffner, D. W. (2000). Pulsed electric fields. *Journal of Food Science*, 65, 65–79. <http://dx.doi.org/10.1111/j.1750-3841.2000.tb00619.x>.
- Boussetta, N., Vorobiev, E., Deloison, V., Pochez, F., Falcimaigne-Cordin, A., & Lanoisellé, J.-L. (2011). Valorisation of grape pomace by the extraction of phenolic antioxidants: application of high voltage electrical discharges. *Food Chemistry*, 128(2), 364–370. <http://dx.doi.org/10.1016/j.foodchem.2011.03.035>.
- Buckow, R., Ng, S., & Toepfl, S. (2013). Pulsed electric field processing of orange juice: A review on microbial, enzymatic, nutritional, and sensory quality and stability. *Comprehensive Reviews in Food Science and Food Safety*, 12(5), 455–467. <http://dx.doi.org/10.1111/1541-4337.12026>.
- Carr, H. Y., & Purcell, E. M. (1954). Effects of diffusion on free precession in nuclear magnetic resonance experiments. *Physical Review*, 94(3), 630–638. <http://dx.doi.org/10.1103/PhysRev.94.630>.
- Ersus, S., & Barrett, D. M. (2010). Determination of membrane integrity in onion tissues treated by pulsed electric fields: Use of microscopic images and ion leakage measurements. *Innovative Food Science & Emerging Technologies*, 11(4), 598–603. <http://dx.doi.org/10.1016/j.ifset.2010.08.001>.
- Faridnia, F., Burritt, D. J., Bremer, P. J., & Oey, I. (2015). Innovative approach to determine the effect of pulsed electric fields on the microstructure of whole potato tubers: Use of cell viability, microscopic images and ionic leakage measurements. *Food Research International*. <http://dx.doi.org/10.1016/j.foodres.2015.08.028>.
- Finley, J. W., Schmidt, S. J., & Serrianni, A. S. (Eds.). (1990). *NMR applications in biopolymers*. Boston, MA: Springer US. <http://dx.doi.org/10.1007/978-1-4684-5868-8>.
- Galindo, F. G., Dejmeck, P., Lundgren, K., Rasmusson, A. G., Vicente, A., & Moritz, T. (2009). Metabolomic evaluation of pulsed electric field-induced stress on potato tissue. *Planta*, 230(3), 469–479. <http://dx.doi.org/10.1007/s00425-009-0950-2>.
- Grimi, N., Mamouni, F., Lebovka, N., Vorobiev, E., & Vaxelaire, J. (2011). Impact of apple processing modes on extracted juice quality: Pressing assisted by pulsed electric fields. *Journal of Food Engineering*, 103(1), 52–61. <http://dx.doi.org/10.1016/j.jfoodeng.2010.09.019>.
- Hjoui, M., & Rubinsky, B. (2010). Magnetic resonance imaging characteristics of nonthermal irreversible electroporation in vegetable tissue. *The Journal of Membrane Biology*, 236(1), 137–146. <http://dx.doi.org/10.1007/s00232-010-9281-2>.
- Ignat, A., Manzocco, L., Brunton, N. P., Nicoli, M. C., & Lyng, J. G. (2014). The effect of pulsed electric field pre-treatments prior to deep-fat frying on quality aspects of potato fries. *Innovative Food Science & Emerging Technologies*, 29, 65–69. <http://dx.doi.org/10.1016/j.ifset.2014.07.003>.
- Ivorra, A., Mir, L. M., & Rubinsky, B. (2009). Electric field redistribution due to conductivity changes during tissue electroporation: Experiments with a simple vegetal model. *IFMBE proceedings*. Vol. 25. (pp. 59–62). <http://dx.doi.org/10.1007/978-3-642-03895-2-18>.
- Jaeger, H., Buechner, C., & Knorr, D. (2012). PEF enhanced drying of plant based products. *Stewart Postharvest Review*, 8(2), 1–7. <http://dx.doi.org/10.2212/spr.2012.2.1>.
- Janositz, A., Noack, A.-K. K., & Knorr, D. (2011). Pulsed electric fields and their impact on the diffusion characteristics of potato slices. *LWT - Food Science and Technology*, 44(9), 1939–1945. <http://dx.doi.org/10.1016/j.lwt.2011.04.006>.
- Jiang, C., Davalos, R. V., & Bischof, J. C. (2015). A review of basic to clinical studies of irreversible electroporation therapy. *IEEE Transactions on Biomedical Engineering*, 62(1), 4–20. <http://dx.doi.org/10.1109/TBME.2014.2367543>.
- Joy, M., Scott, G., & Henkelman, M. (1989). In vivo detection of applied electric currents by magnetic-resonance imaging. *Magnetic Resonance Imaging*, 7(1), 89–94.
- Khang, H. S., Lee, B. Il, Oh, S. H., Woo, E. J., Lee, S. Y., Cho, M. H., ... Seo, J. K. (2002). J-substitution algorithm in magnetic resonance electrical impedance tomography (MREIT): Phantom experiments for static resistivity images. *IEEE Transactions on Medical Imaging*, 21(6), 695–702. <http://dx.doi.org/10.1109/TMI.2002.800604>.
- Kim, H. J., Kim, Y. T., Minhas, A. S., Jeong, W. C., Woo, E. J., Seo, J. K., & Kwon, O. J. (2009). In vivo high-resolution conductivity imaging of the human leg using MREIT: The first human experiment. *IEEE Transactions on Medical Imaging*, 28(11), 1681–1687. <http://dx.doi.org/10.1109/TMI.2009.2018112>.
- Kotnik, T., Kramar, P., Pucihar, G., Miklavčič, D., & Tarek, M. (2012). Cell membrane electroporation – Part 1: The phenomenon. *IEEE Electrical Insulation Magazine*, 28(5), 14–23. <http://dx.doi.org/10.1109/MEI.2012.6268438>.
- Kranjc, M., Bajd, F., Serša, I., & Miklavčič, D. (2011). Magnetic resonance electrical impedance tomography for monitoring electric field distribution during tissue electroporation. *IEEE Transactions on Medical Imaging*, 30(10), 1771–1778. <http://dx.doi.org/10.1109/TMI.2011.2147328>.
- Kranjc, M., Bajd, F., Serša, I., & Miklavčič, D. (2014). Magnetic resonance electrical impedance tomography for measuring electrical conductivity during electroporation. *Physiological Measurement*, 35(6), 985–996. <http://dx.doi.org/10.1088/0967-3334/35/6/985>.
- Kranjc, M., Bajd, F., Serša, I., Woo, E. J., & Miklavčič, D. (2012). Ex vivo and in silico feasibility study of monitoring electric field distribution in tissue during electroporation based treatments. *PLoS One*, 7(9), e45737. <http://dx.doi.org/10.1371/journal.pone.0045737>.
- Kranjc, M., Markelc, B., Bajd, F., Čemažar, M., Serša, I., Blagus, T., & Miklavčič, D. (2015). In situ monitoring of electric field distribution in mouse tumor during electroporation. *Radiology*, 274(1), 115–123. <http://dx.doi.org/10.1148/radiol.14140311>.
- Mahnič-Kalamiza, S., Vorobiev, E., & Miklavčič, D. (2014). Electroporation in food processing and biorefinery. *The Journal of Membrane Biology*, 247(12), 1279–1304. <http://dx.doi.org/10.1007/s00232-014-9737-x>.
- Miklavčič, D., Beravs, K., Semrov, D., Čemažar, M., Demšar, F., & Serša, G. (1998). The importance of electric field distribution for effective in vivo electroporation of tissues. *Biophysical Journal*, 74(5), 2152–2158.
- Nott, K. P., Shaarani, S. M., & Hall, L. D. (2003). The effect of microwave heating on potato texture studied with magnetic resonance imaging. *Magnetic resonance in food science* (pp. 38–45). Cambridge: Royal Society of Chemistry. <http://dx.doi.org/10.1039/9781847551269-00038>.
- Phoon, P. Y., Galindo, F. G., Vicente, A., & Dejmeck, P. (2008). Pulsed electric field in combination with vacuum impregnation with trehalose improves the freezing tolerance of spinach leaves. *Journal of Food Engineering*, 88(1), 144–148. <http://dx.doi.org/10.1016/j.jfoodeng.2007.12.016>.
- Raso, J., & Heinz, V. (Eds.). (2006). *Pulsed electric fields technology for the food industry*. Boston, MA: Springer US. <http://dx.doi.org/10.1007/978-0-387-31122-7>.
- Raso, J., Calderón, M. L., Góngora, M., Barbosa-Cánovas, G., & Swanson, B. G. (1998). Inactivation of mold asporospores and conidiospores suspended in fruit juices by pulsed electric fields. *LWT - Food Science and Technology*, 31(7–8), 668–672. <http://dx.doi.org/10.1006/ftsl.1998.0426>.
- Rols, M. P., & Teissié, J. (1990). Electroporation of mammalian cells. Quantitative analysis of the phenomenon. *Biophysical Journal*, 58(5), 1089–1098. [http://dx.doi.org/10.1016/S0006-3495\(90\)82451-6](http://dx.doi.org/10.1016/S0006-3495(90)82451-6).
- Seo, J. K., & Woo, E. J. (2014). Electrical tissue property imaging at low frequency using MREIT. *IEEE Transactions on Biomedical Engineering*, 61(5), 1390–1399. <http://dx.doi.org/10.1109/TBME.2014.2298859>.
- Serša, I., Jarh, O., & Demšar, F. (1994). Magnetic resonance microscopy of electric currents. *Journal of Magnetic Resonance, Series A*, 111(1), 93–99. <http://dx.doi.org/10.1006/jmra.1994.1230>.
- Serša, I., Kranjc, M., & Miklavčič, D. (2015). Current density imaging sequence for monitoring current distribution during delivery of electric pulses in irreversible electroporation. *Biomedical Engineering Online*, 14(Suppl. 3), S6. <http://dx.doi.org/10.1186/1475-925X-14-S3-S6>.
- Stejskal, E. O., & Tanner, J. E. (1965). Spin diffusion measurements: Spin echoes in the presence of a time-dependent field gradient. *The Journal of Chemical Physics*, 42(1), 288. <http://dx.doi.org/10.1063/1.1695690>.
- Toepfl, S. (2011). Pulsed electric field food treatment – Scale up from lab to industrial scale. *Procedia Food Science*, 1, 776–779. <http://dx.doi.org/10.1016/j.profoo.2011.09.117>.
- Tsong, T. Y. (1991). Electroporation of cell membranes. *Biophysical Journal*, 60(2), 297–306. [http://dx.doi.org/10.1016/S0006-3495\(91\)82054-9](http://dx.doi.org/10.1016/S0006-3495(91)82054-9).
- van Everdingen, K. J., van der Grond, J., Kappelle, L. J., Ramos, L. M., & Mali, W. P. (1998). Diffusion-weighted magnetic resonance imaging in acute stroke. *Stroke*, 29(9), 1783–1790.
- Vidmar, J., Kralj, E., Bajd, F., & Serša, I. (2015). Multiparametric MRI in characterizing venous thrombi and pulmonary thromboemboli acquired from patients with pulmonary embolism. *Journal of Magnetic Resonance Imaging*, 42(2), 354–361. <http://dx.doi.org/10.1002/jmri.24816>.
- Vorobiev, E., & Lebovka, N. (2010). Enhanced extraction from solid foods and biosuspensions by pulsed electrical energy. *Food Engineering Reviews*, 2(2), 95–108. <http://dx.doi.org/10.1007/s12393-010-9021-5>.
- Yarmush, M. L., Golberg, A., Serša, G., Kotnik, T., & Miklavčič, D. (2014). Electroporation-based technologies for medicine: Principles, applications, and challenges. *Annual Review of Biomedical Engineering*, 16(1), 295–320. <http://dx.doi.org/10.1146/annurev-bioeng-071813-104622>.